

# Biotin-tagged fluorescent sensor to visualize 'mobile' Zn<sup>2+</sup> in cancer cells

Le Fang,<sup>a</sup> Giuseppe Trigiante,<sup>b</sup> Christina J. Kousseff,<sup>a</sup> Rachel Crespo-Otero,<sup>a</sup> Michael P. Philpott,<sup>b</sup> and Michael Watkinson<sup>\*a,c</sup>

a. The Joseph Priestley Building, School of Biological and Chemical Sciences, Queen Mary University of London, Mile End Road, London, E1 4NS, UK.

b. Centre for Cutaneous Research, Institute of Cell and Molecular Science, Barts and The London School of Medicine and Dentistry, Queen Mary University of London, London E1 2AT, UK.

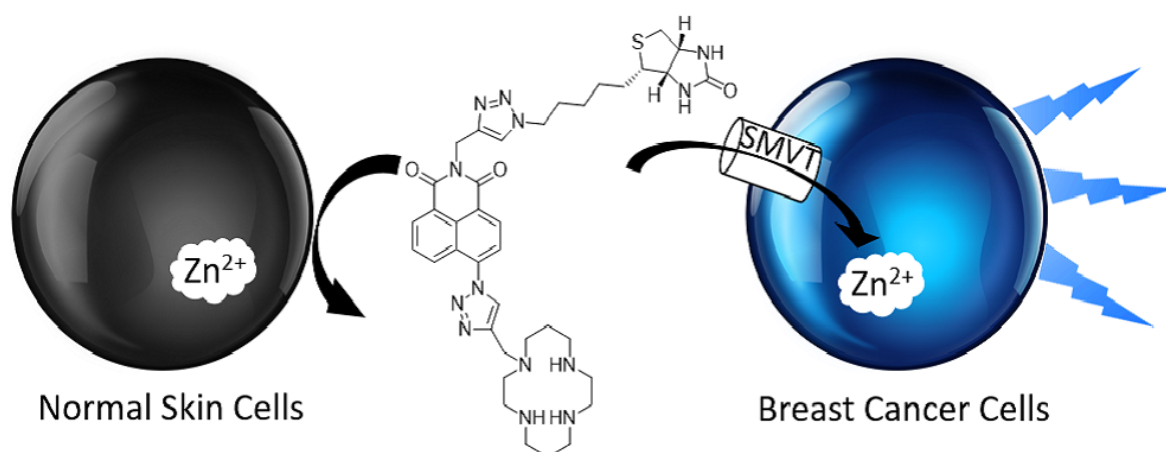
c. The Lennard-Jones Laboratories, School of Chemical and Physical Science, Keele University, ST5 5BG, UK. Email: [m.watkinson@keele.ac.uk](mailto:m.watkinson@keele.ac.uk)

Received 5<sup>th</sup> July 2018,

Accepted 27<sup>th</sup> July 2018,

DOI: 10.1039/C8CC05425H

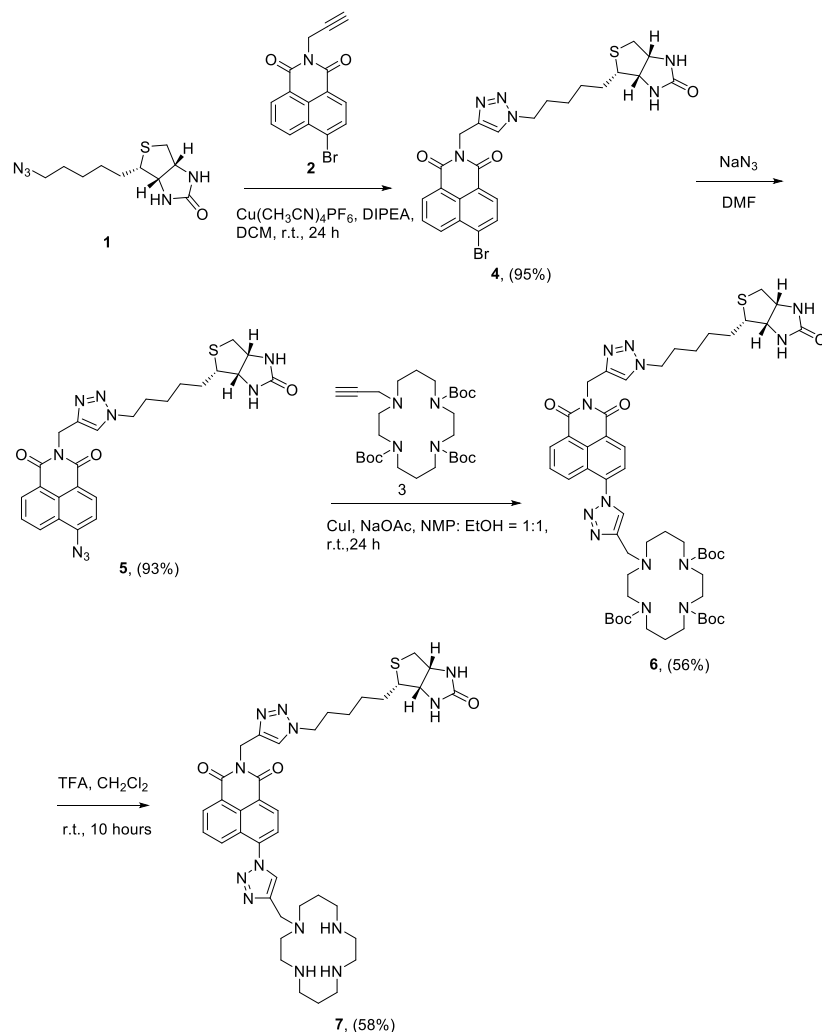
**Abstract:** A cancer cell-targeting fluorescent sensor has been developed to image mobile Zn<sup>2+</sup> by introducing a biotin group. It shows a highly selective response to Zn<sup>2+</sup> in vitro, no toxicity in cellulo and images 'mobile' Zn<sup>2+</sup> specifically in cancer cells. We believe this probe has the potential to help improve our understanding of the role of Zn<sup>2+</sup> in the processes of cancer initiation and development.



Zinc, as the second most abundant d-block metal in the human body, plays an important role in many biological processes.<sup>1</sup> The aberration of zinc levels, which can cause the dysfunction of these processes, is related to a wide range of diseases.<sup>2</sup> One of these diseases, cancer, causes millions of deaths every year and is a major burden of disease around the world. There is evidence that zinc is important in cancer development.<sup>3</sup> This is perhaps unsurprising as zinc is necessary for the human superoxide dismutase enzyme system to function, and cancer cells are highly dependent on superoxide dismutase for protecting themselves from the damage induced by reactive oxygen species, since the superoxide anion radical,  $O_2^{\cdot-}$ , is actively produced in cancer cells.<sup>4</sup> Zinc is also a growth factor in cell proliferation,<sup>5</sup> which is attenuated in the absence of zinc.<sup>6</sup> However, it is found that the alterations of mobile zinc concentration in malignant cells are tissue specific. For example, zinc concentration increases by about 72% in breast cancer tissue,<sup>7</sup> while it decreases by 75% in malignant prostate tissue<sup>8</sup> compared to their non-cancerous counterparts. These difference have been explained by changes in expression of zinc transporters, which directly influence the  $Zn^{2+}$  cellular influx and efflux.<sup>9</sup> In prostate cancer, the low  $Zn^{2+}$  concentration is due to the downregulation of the zinc transporter ZIP1,<sup>8</sup> whilst ZIP6<sup>10</sup>, ZIP7<sup>11</sup> and ZIP10<sup>12</sup> have been proposed to be important in the elevated levels in breast cancer. Though there is an increasing understanding of these processes, it is still unclear whether these changes are a cause or an effect of the cancer. Furthermore, it is not clear whether zinc itself or zinc transporters are associated with the cancer-related events.<sup>3</sup> However, the difficulty of imaging *in vivo* represents a significant barrier to understanding its role in cancer. Therefore, the development of an effective way to detect mobile zinc specifically in tumour cells would allow us to achieve a better understanding of its role in the mechanism of cancer initiation, progression, and potentially, its prevention.

Small molecule fluorescent sensors, which can image  $Zn^{2+}$  with fluorescence as their output have become one of the most predominant methods in use today due to their high sensitivity, low toxicity, and good photophysical properties.<sup>13,14</sup> We have developed a modular double 'click' synthetic methodology to produce biologically targeted  $Zn^{2+}$  sensors for both extracellular and intracellular imaging of zinc.<sup>15</sup> Biotin is a vitamin essential to cancer cells and the sodium-dependent multi-vitamin transporter (SMVT) is overexpressed in many cancers, including breast, lung, ovarian, mastocytoma and renal,<sup>16</sup> meaning that cancer cells uptake more biotin than normal cells. Based on this, some biotin tagged cancer drugs have been developed and have shown good targeting.<sup>17</sup> We therefore hypothesized that by incorporating a biotin tag into a zinc probe, using our previously reported methodology, we could generate a small molecule probe that could detect zinc specifically.

The cyclam ligand has previously been shown to be an effective receptor unit for mobile zinc,<sup>18</sup> and was therefore chosen in this study. The synthetic route to the target probe, **7**, is shown in Scheme 1. Biotin azide, **1**, was prepared from D-(+)-biotin by adapting literature procedures (see Electronic Supplementary Information).<sup>19</sup> The fluorophore and ligand were introduced via alkynes **2** and **3**, which were synthesized using the procedure we reported previously.<sup>15,18</sup> After double click reactions,<sup>20</sup> the Boc-protected **6** was isolated in moderate yield and was de-protected under standard conditions to give sensor **7** (see ESI). Unless otherwise noted, all photophysical experiments in solution were performed in 0.01 mM aqueous HEPES buffer at pH 7.4 and  $ZnCl_2$  was chosen as the binding metal ion source, in order to simulate the chloride-rich biological environment.



Scheme 1 The synthetic route to sensor **7**.

The Job plot clearly showed the expected  $\text{Zn}^{2+}$ :**7** binding stoichiometry of 1:1, (see ESI, Fig. S2). This binding behaviour has also been studied using DFT calculations. The optimized structure of the complex of **7** with 1 equivalent  $\text{Zn}^{2+}$  in water revealed the expected structure involving ligation of the cyclam nitrogen donors with the triazole ligand acting as a scorpion-like donor (Fig. S8, ESI), and is similar to the single crystal X-ray structure of a closely related analogue.<sup>18</sup>

The fluorescence of **7** is switched on by adding  $\text{Zn}^{2+}$  and is based on a mechanism restricting intramolecular vibrations (see ESI, Fig. S9). As shown in Fig 1a, upon addition of  $\text{Zn}^{2+}$ , the fluorescence intensity increased gradually with an approximately 5-fold maximum increase. The dissociation constant with  $\text{Zn}^{2+}$  was measured through non-linear curve fitting and was determined to be  $1.88 \times 10^{-8}$  M. The quantum yield of **7** was found to be 0.02, while this increased to 0.05 after binding to 1 equivalent of  $\text{Zn}^{2+}$ . Although this is rather modest, it is in line with previous measurements<sup>18</sup> and we have shown such probes to be tractable in biological milieu.

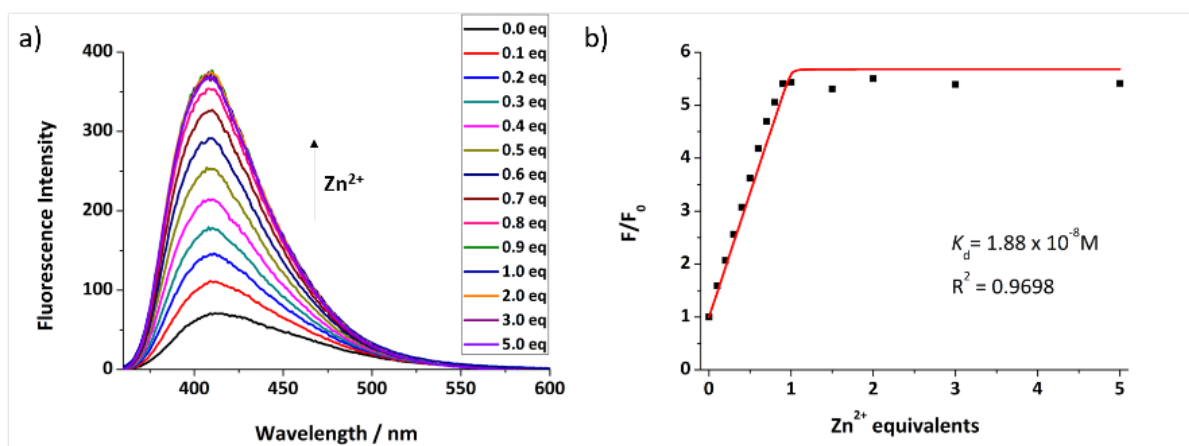


Fig. 1 a) The fluorescence switch-on response of sensor **7** (50  $\mu$ M) to different equivalents  $\text{Zn}^{2+}$  in 0.01 mM HEPES buffer ( $\lambda_{\text{ex}} = 346$  nm,  $\lambda_{\text{em}} = 412$  nm, slit width: 5 nm); b) the non-linear curve fitting of the fluorescence intensity against different equivalents  $\text{Zn}^{2+}$ .

The pH-dependent fluorescence response was measured, as it is known that although cancer cells maintain their pH near to neutrality, they are more acidic than normal cells.<sup>21</sup> As shown in Fig. 2a, sensor **7** shows a good switch-on response to 1 equivalent  $\text{Zn}^{2+}$  in the range of pH 5.5-10.5, indicating that it should be able to detect  $\text{Zn}^{2+}$  in most cancer cells. The apparent  $\text{pK}_{\text{a}}$  of **7** was measured by integrating the fluorescence intensity of emission spectra against pH (see ESI, Fig. S4). Through non-linear curve fitting (see ESI, Equation S3), the four apparent  $\text{pK}_{\text{a}}$ s of **7** are:  $\text{pK}_{\text{a}1} = 1.64 \pm 0.14$ ,  $\text{pK}_{\text{a}2} = 4.18 \pm 0.23$ ,  $\text{pK}_{\text{a}3} = 9.24 \pm 0.31$ ,  $\text{pK}_{\text{a}4} = 11.18 \pm 0.18$ .

The selectivity of sensor **7** to  $\text{Zn}^{2+}$  over other competing metal ions was also investigated. As shown in Fig. 2b, besides  $\text{Zn}^{2+}$ , the fluorescence is not switched on after the addition of other metal ions, with the exception of  $\text{Cd}^{2+}$ , which shows a smaller response in line with our previous findings.<sup>18</sup> However, as its concentration in tissues is negligible this is not an issue. Whilst  $\text{Fe}^{3+}$ ,  $\text{Co}^{2+}$  and  $\text{Cu}^{2+}$  induce significant quenching<sup>22</sup> of the fluorescence of **7**, they almost exclusively exist in bound forms in biology, rather than as the free cations tested here. The cations  $\text{Na}^+$ ,  $\text{K}^+$ ,  $\text{Ca}^{2+}$ , and  $\text{Mg}^{2+}$ , which are the main metal ions in cells, showed no effect on the fluorescence intensity of sensor **7**, meaning that it should have good selectivity for  $\text{Zn}^{2+}$  and can potentially be applied *in cellulo*. The water-solubility of **7** is also an attractive feature for cell imaging as it does not require the addition of co-organic solvents to solubilize the probe.

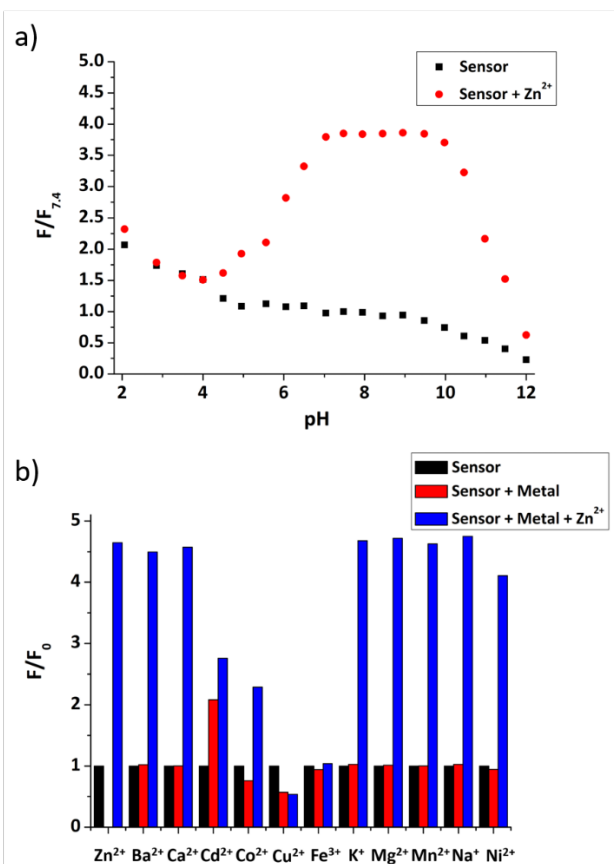


Fig. 2 a) The pH profile of **7** (50  $\mu$ M) and **7** with 1 equivalent  $\text{Zn}^{2+}$  in 0.01 mM HEPES buffer. b) Metal ion selectivity of **7**. Average normalized fluorescence intensities for 50  $\mu$ M **7** in buffer (0.01 mM HEPES, pH 7.4) (black bars), after addition of 5 equivalents of various metal ions (red bars), followed by addition of 1 equivalent  $\text{ZnCl}_2$  (blue bars).

With these promising properties confirmed *in vitro*, the innate toxicity of sensor **7** was then measured. The MCF-7 breast cancer and N-TERT keratinocytes cell lines were incubated in cell medium solution containing different concentrations of **7** for 24 hours. Then the solution was washed away and alamarBlue was added as an indicator of cell health.<sup>23</sup> From these experiments (see ESI, Table S1), we can conclude that the sensor has no toxicity to either cell type, since the number of living cells does not decrease as the concentration of sensor increases.

Confocal fluorescence microscopy was used to detect mobile  $\text{Zn}^{2+}$  in MCF-7 and N-TERT keratinocytes cells and the results are shown in Fig. 3 (see also ESI, Fig. S7). For MCF-7 breast cancer cells, when there was no sensor, the fluorescence of the cells was very weak, resulting from their background autofluorescence. After incubation with a 100  $\mu$ M solution of **7** for 2 hours, the fluorescence increased considerably, and the cytoplasm can be visualized clearly, but there was no response from the nucleus. On the addition of zinc pyrithione, a membrane permeable zinc source,<sup>24</sup> the fluorescence response of the cells became stronger and a fluorescence response was observed from the whole cell, including the nucleus. We therefore assume that this sensor is also permeable to the nucleus, but that the concentration of nuclear mobile zinc in MCF-7 cells is very low. When TPEN, a well-known zinc chelator,<sup>25</sup> was added to remove  $\text{Zn}^{2+}$  inside cells, the fluorescence of the cells decreased markedly as expected. Pleasingly, as hypothesized, for the normal control N-TERT keratinocytes cells, we observed no strong fluorescence response even after the addition of zinc pyrithione (Fig. S7, ESI), confirming the selective localization of sensor **7** in the cancer cells.

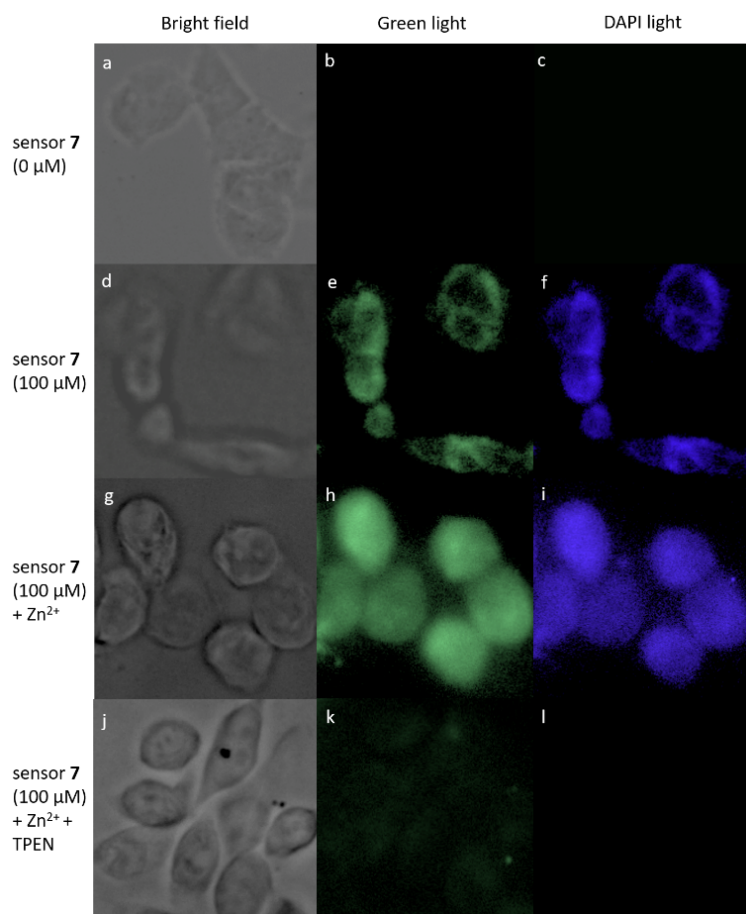


Fig. 3 Confocal microscopy images of MCF-7 cells treated with no sensor (a-c), 100  $\mu\text{M}$  sensor **7** solution (d-f), sensor **7** (100  $\mu\text{M}$ ) with saturated zinc pyrithione (g-i), and sensor **7** (100  $\mu\text{M}$ ) after loading the cells with zinc pyrithione, then TPEN (2  $\mu\text{M}$ ) was added (j-l).

In conclusion, the biotin tagged fluorescent sensor was developed using a double click reaction. It is water soluble, and has high selectivity, low toxicity, shows good fluorescence response and a low dissociation constant to  $\text{Zn}^{2+}$ . Testing in cells confirms it can localize selectively in cancer cells, can image mobile  $\text{Zn}^{2+}$ , and therefore has potential to help us better understand the role of  $\text{Zn}^{2+}$  in cancer initiation and progressio

### Conflicts of interest

There are no conflicts of interest to declare.

### Acknowledgements

We acknowledge the EPSRC National Mass Spectrometry Service, University of Wales, Swansea for the provision of high resolution mass spectrometry. TDDFT calculations were performed on the QMUL Apocrita facility. We are grateful to the Chinese Scholarship Council (LF) and the EPSRC (CK) for the provision of PhD studentships.

### Notes and references

- 1 Y. Chen, Y. Bai, Z. Han, W. He and Z. Guo, *Chem. Soc. Rev.*, 2015, **44**, 4517-4546.
- 2 a) A. I. Bush, W. H. Pettingell, G. Multhaup, M. D. Paradis, J.-P. Vonsattel, J. F. Gusella, K. Beyreuther, C. L. Masters and R. E. Tanzi, *Science*, 1994, **265**, 1464-1467; b) C. J. Frederickson, J.-Y. Koh and A. I. Bush, *Nat. Rev. Neurosci.*, 2005, **6**, 449-462; c) M. Cortesi, R. Chechik, A.

- Breskin, D. Vartsky, J. Ramon, G. Raviv, A. Volkov and E. Fridman, *Phys. Med. Biol.*, 2009, **54**, 781-796.
- 3 B. J. Grattan and H. C. Freake, *Nutrients*, 2012, **4**, 648-675.
  - 4 P. Huang, L. Feng, E. A. Oldham, M. J. Keating and W. Plunkett, *Nature*, 2000, **407**, 390-395.
  - 5 S. C. Paski and Z. Xu, *Can. J. Physiol. Pharmacol.*, 2002, **80**, 790-795.
  - 6 A. S. Prasad, F. W. J. Beck, L. Endre, W. Handschu, M. Kukuruga and G. Kumar, *J. Lab. Clin. Med.*, 1996, **128**, 51-60.
  - 7 E. J. Margalioth, J. G. Schenker, M. Chevion and E. J. Margalioth, *Cancer*, 1983, **52**, 868-872.
  - 8 R. B. Franklin, P. Feng, B. Milon, M. M. Desouki, K. K. Singh, A. Kajdacsy-Balla, O. Bagasra and L. C. Costello, *Mol. Cancer*, 2005, **4**, 1-13.
  - 9 a) W. Maret, *Biometals*, 2001, **14**, 187-190; b) D. J. Eide, *Pflugers Arch. Eur. J. Physiol.*, 2004, **447**, 796-800.
  - 10 M. Chihiro, T. Tomoka, H. Yuki, K. Satomi, N. Ikuhiko and T. Koichi, *FEBS Lett.*, 2017, **591**, 3348-3359.
  - 11 K. M. Taylor, P. Vichova, N. Jordan, S. Hiscox, R. Hendley and R. I. Nicholson, *Endocrinology*, 2008, **149**, 4912-4920.
  - 12 N. Kagara, N. Tanaka, S. Noguchi and T. Hirano, *Cancer Sci.*, 2007, **98**, 692-697.
  - 13 For selected review articles see: a) Z. Xu, J. Yoon and D. R. Spring, *Chem. Soc. Rev.*, 2010, **39**, 1996-2006; b) E. M. Nolan and S. J. Lippard, *Acc. Chem. Res.*, 2009, **42**, 193-203; c) K. P. Carter, A. M. Young and A. E. Palmer, *Chem. Rev.*, 2014, **114**, 4564-4601; d) J. A. Drewry and P. T. Gunning, *Coord. Chem. Rev.*, 2011, **255**, 459-472; e) H. M. Kim and B. R. Cho, *Chem. Rev.*, 2015, **115**, 5014-5055; f) E. M. Nolan and S. J. Lippard, *Acc. Chem. Res.*, 2008, **42**, 193-203; g) D. Wu, A. C. Sedgwick, T. Gunnlaugsson, E. U. Akkaya, J. Yoon and T. D. James, *Chem. Soc. Rev.*, 2017, **46**, 7105-7123.
  - 14 For recent examples of small molecule zinc sensors see: a) J. M. Goldberg, F. Wang, C. D. Sessler, N. W. Vogler, D. Y. Zhang, W. H. Loucks, T. Tzounopoulos and S. J. Lippard, *J. Am. Chem. Soc.*, 2018, **140**, 2020-2023; b) X. Yan, J. J. Kim, H. S. Jeong, Y. K. Moon, Y. K. Cho, S. Ahn, S. B. Jun, H. Kim and Y. You, *Inorg. Chem.*, 2017, **56**, 4332-4346; c) H. Mehdi, W. Gong, H. Guo, M. Watkinson, H. Ma, A. Wajahat and G. Ning, *Chem. - A Eur. J.*, 2017, **23**, 13067-13075.
  - 15 J. Pancholi, D. J. Hodson, K. Jobe, G. A. Rutter, S. M. Goldup and M. Watkinson, *Chem. Sci.*, 2014, **5**, 3528-3535.
  - 16 a) J.-F. Shi, P. Wu, Z.-H. Jiang and X.-Y. Wei, *Eur. J. Med. Chem.*, 2014, **71**, 219-228; b) A. Doerflinger, N. N. Quang, E. Gravel, G. Pinna, M. Vandamme, F. Duconge and E. Doris, *Chem. Commun.*, 2018, **54**, 3613-3616.
  - 17 a) S. Chen, X. Zhao, J. Chen, J. Chen, L. Kuznetsova and S. S. Wong, *Bioconjug. Chem.*, 2010, **21**, 979-987; b) S. Maiti, N. Park, J. H. Han, H. M. Jeon, J. H. Lee, S. Bhuniya, C. Kang and J. S. Kim, *J. Am. Chem. Soc.*, 2013, **135**, 4567-4572; c) G. Tripodo, D. Mandracchia, S. Collina, M. Rui and D. Rossi, *Med. Chem.*, 2014, DOI: 10.4172/2161-0444.S1-004; d) T. Kim, H. M. Jeon, H. T. Le, T. W. Kim, C. Kang and J. S. Kim, *Chem. Commun.*, 2014, **50**, 7690-7693; e) N. Muhammad, N. Sadia, C. Zhu, C. Luo, Z. Guo and X. Wang, *Chem. Commun.*, 2017, **53**, 9971-9974.
  - 18 E. Tamanini, A. Katewa, L. M. Sedger, M. H. Todd and M. Watkinson, *Inorg. Chem.*, 2009, **48**, 319-324; b) E. Tamanini, A. Katewa, L. Sedger, M. H. Todd and M. Watkinson, *Inorg. Chem.*, 2009, **48**, 319-324; c) K. Jobe, C. H. Brennan, M. Motevalli, S. M. Goldup, and M. Watkinson, *Chem. Commun.*, 2011, **47**, 6036-6038.
  - 19 a) C. Corona, B. K. Bryant and J. B. Arterburn, *Org. Lett.*, 2006, **8**, 1883-1886; b) D. James, J. M. Escudier, E. Amigues, J. Schulz, C. Vitry, T. Bordenave, M. Szlosek-Pinaud and E. Fouquet, *Tetrahedron Lett.*, 2010, **51**, 1230-1232.
  - 20 In the present study it was found that a stepwise synthesis was more effective than the previously reported one-pot procedure. Although this does work, the product is contaminated by a number of by-products and required protracted purification by column chromatography. In contrast the stepwise procedure only required purification by recrystallisation.
  - 21 J. R. Griffiths, *Br. J. Cancer*, 1991, **64**, 425-427.
  - 22 C. Ripoll, M. Martin, M. Roldan, E. M. Talavera, A. Orte and M. J. Ruedas-Rama, *Chem. Commun.*, 2015, **51**, 16964-16967.
  - 23 J. O'Brien, I. Wilson, T. Orton and F. Pognan, *Eur. J. Biochem.*, 2000, **267**, 5421-5426.
  - 24 W. Q. Ding and S. E. Lind, *IUBMB Life*, 2009, **61**, 1013-1018.
  - 25 P. Jiang and Z. Guo, *Coord. Chem. Rev.*, 2004, **248**, 205-229.